Optical properties of liquid silicon: the integral equation approach

Monika S K Fuchs†

Institute of Technical Physics, DLR Stuttgart, Pfaffenwaldring 38–40, 70569 Stuttgart, Germany

Abstract. A calculation of the optical conductivity and related optical properties of liquid silicon is presented. Starting from the results of a single superchain/effective medium approximation for the electronic properties, the frequency dependent conductivity is evaluated in terms of the Kubo–Greenwood formula. For a fast computation of the three and four centre terms therein the effective handling of the angular dependences of the Green's functions known from the sp^3-fluid model is generalized to the current matrix elements. A good agreement of our results with experimental data for liquid silicon is found. At higher frequencies (>5 eV) and in the fitted Drude parameters, however, there are discrepancies due to the limitations of the sp^3-model.

1. Introduction

Less theoretical work is done on the optical properties of molten systems like liquid silicon [1,2] than on the mostly computed electronic density of states [2–9], although the optical properties are of more practical interest and more tractable from the experimental point of view [10–19] than the electronic ones [20–22]. The knowledge, especially of the change in optical constants during the melting phase transition, can be advantageous in many technological applications, e.g., for controlling the growth of single crystals from the melt or if very short laser pulses are used for melting. In this case the optical observation method will be the only one which is able to resolve changes on such short time scales.

The aim of this paper is to extend the powerful integral equation methods and its advantages (no statistical errors, less numerical effort than in molecular dynamics) to the calculation of optical properties. Starting from the integral equation approach given by the single superchain/effective medium approximation (SSCA/EMA) for the electronic density of states and the continuum (i.e. ensemble averaged) Green functions of the sp^3 model of liquid silicon, the optical properties are determined via the Kubo–Greenwood formula. In its formulation in terms of matrix elements of the Green function in general not only the diagonal parts contribute to the conductivity and therefore one has to evaluate multiple integrals connecting (non-diagonal) Green functions and optical matrix elements. The deduction of the equation for the optical conductivity consistent with the SSCA/EMA is the topic of section 2.

Even without vertex corrections the dependence on the angular variables describing the orientations of the basis orbitals with respect to the distance vector of the two atoms involved has to be extended to the direction of the electric field vector of the incoming light. The handling of these angular dependences will be treated in section 3.

† Present address: Technische Universität München, Fachgebiet für Theoretische Chemie, Lichtenbergstraße 4, 85747 Garching, Germany.

The results of this continuum Green function method for the optical properties of liquid silicon as a sp³-fluid are presented in section 4. They agree well with various experimental data from ellipsometry or angle-dependent reflectivity measurements. Especially in the low-frequency limit the magnitude of the conductivity is more consistent with experimental data than previous molecular dynamics results which deviate by a factor of 1.5 [2] or 0.3 [1]. In the high-frequency region, however, deviations occur because of the limited validity of the sp³-model used. This also has consequences for the real part of the dielectric function because an extrapolation is needed to use the Kramers–Kronig transformation. Better results are expected to be determined from an spd-basis, as discussed in the end of section 4.

2. Optical conductivity in terms of continuum Green functions

Integral equation methods like the SSCA/EMA immediately yield diagonal and non-diagonal continuum (i.e. ensemble averaged) Green functions [23,24]. In general, with the knowledge of Green function matrix elements (for a given configuration) and some optical matrix elements (e.g. matrix elements of the momentum or of the current operator) one can use the Kubo–Greenwood formula to determine the optical conductivity. After some manipulations (see [25, 26]) it becomes

$$\sigma(\omega) = \frac{\pi \hbar}{\Omega} \sum_{\mu\nu} J^z_{\mu\nu} J^z_{\nu\mu} \frac{\exp(-\beta\hbar\omega) - 1}{\hbar\omega}$$

$$\times \int dE f_T(E) \left(1 - f_T(E + \hbar\omega)\right) \delta(E - \epsilon_\mu) \delta(E - \epsilon_\nu + \hbar\omega) \tag{1}$$

where f_T is the Fermi distribution function at temperature T, $\beta = 1/kT$ and Ω the volume of the system. The indices μ, ν in (1) denote the eigenfunctions to the eigenvalues ϵ of the system and $J^z_{\mu\nu}$ is the corresponding matrix element of the operator of the current in an arbitrary but fixed direction z. Of course, for an isotropic liquid the conductivity can be treated as a scalar. The index z is only for reminding that both current matrix elements belong to the same direction. Replacing the δ-functions in (1) in terms of Green functions ($\delta(E - \epsilon_\mu) = \text{Im}G_{\mu\mu}(E - i0)/(n\pi)$ where n is the total number of states in the system) one gets an expression that includes the trace of the following operator:

$$(J\text{Im}G(E + \hbar\omega)J\text{Im}G(E)).$$

Within a given tight binding basis (consisting of elements labeled i, j etc) one can express the Green operator by $G = \sum_{i,j} |i\rangle \check{G}_{ij} \langle j|$, and therefore the conductivity is given by

$$\sigma(\omega) = \frac{\hbar\rho}{\pi} \frac{\exp(-\beta\hbar\omega) - 1}{\hbar\omega} \int dE f_T(E) \left(1 - f_T(E + \hbar\omega)\right)$$

$$\times \left[\frac{1}{N} \sum_{ijkl} J_{ij} \text{Im}\check{G}_{jk}(E + \hbar\omega) J_{kl} \text{Im}\check{G}_{li}(E) \right] \tag{2}$$

where ρ is the number density of atoms and N is their total number. This formula is independent of whether the elements of the basis are orthogonal to each other or not. Until now a concrete configuration of atoms was considered, but what we are interested in is the ensemble average. Except for a phenomenological correction, no vertex corrections are taken into account for further evaluation, i.e., for the average over the product of Green functions the approximation

$$\langle \text{Im}\check{G}_{jk}(E + \hbar\omega) \text{Im}\check{G}_{li}(E) \rangle = \langle \text{Im}\check{G}_{jk}(E + \hbar\omega) \rangle \langle \text{Im}\check{G}_{li}(E) \rangle$$

is used. This is a good approximation in the case of metals [23, 25, 27]. A method of how to consider a full vertex correction may be derived in a similar way as in [28–30], but this would

require another self-consistent calculation at every pair of energies, so the advantage of the integral equation methods to need less numerical effort would break down.

For the averaged values of the Green function matrix elements $G_{ij}(\boldsymbol{r}) = \langle \check{G}_{ij}\delta(\boldsymbol{R}_i - \boldsymbol{R}_j - \boldsymbol{r})\rangle$ (where $\boldsymbol{R}_i$ is the atomic centre corresponding to basis function i) the continuum Green functions (diagonal and non-diagonal) resulting from the SSCA/EMA [8, 32, 33] are used. To evaluate the ensemble average of the fourfold summation term one has to distinguish some cases, depending on how many and which of the four contributing atomic places are identical [25].

In the following we will consider the terms yielding the ensemble average of the term in square brackets in (2). Each summation index therein can be divided, one labelling the position where the basis orbital is centred and the other labelling all other characteristics of the orbital, e.g. the orbital quantum number. Because the averaging process refers only to the atomic centres we assume for simplicity as a first step only one basis function per atom and suppress the second kind of index. In the general case however, the fourfold summation over these indices remain. We will come back to this at the end of this section.

For further abbreviation, an upper index i for the imaginary part is used and the bar ($\bar{G}$) denotes the diagonal part of the Green function. To distinguish between the two energies (E and $E' = E + \hbar\omega$) G and G' are used and the explicit dependence on the energy is suppressed in the notation. For the introduction of a phenomenological vertex correction we have to make some remarks: In the SSCA/EMA (and some other integral equation methods) the continuum non-diagonal Green function contains the pair distribution function $g(r)$ as a factor [23,31]. Following from that a function $A(\boldsymbol{r})$ can be defined such that $G(\boldsymbol{r}) = g(r)A(\boldsymbol{r})$ holds. The distribution functions describing the probability of finding the atoms in (2) in a certain configuration have to be approximated by pair distribution functions. To do this in a consistent way with the approximations inherent in the SSCA/EMA [23], one has to consider the following points. (i) As mentioned above, $G(\boldsymbol{r})$ already contains the pair distribution, so one has to ensure that it is not taken twice. (ii) For the two centre terms it follows from (i) that if $G(\boldsymbol{r})$ occurs, no extra $g(r)$ has to be taken into account, and if $G(\boldsymbol{r})G(-\boldsymbol{r})$ would occur one has to replace one of the G's by the above defined function A. (iii) The three particle distribution function in the SSCA/EMA is simply a chain of pair distribution functions connecting each pair in the three particles. Analogous to the two centre terms, if $G(\boldsymbol{r})$ occurs, no extra $g(r)$ has to be taken into account. Only the matrix elements of the current $J(\boldsymbol{r})$ (as a function of the distance vector of the two centres) has to be weighted with $g(r)$. (iv) The approximation of the four particle distribution function in the SSCA/EMA can be written in three additive terms: The first one is a pure chain connecting successive pairs of points and the last with the first one, the second and third terms contain this chain with an additional factor $h(r) = g(r) - 1$ connecting two diagonal points in each case.

Abiding by these rules, one gets the following terms:

● one centre term:

$$\bar{G}^i J(0)\bar{G}^{i\prime} J(0)$$

● two centre terms:

$$\rho \int \bar{G}^i J(\boldsymbol{r})\bar{G}^{i\prime} J(-\boldsymbol{r})g(r)\mathrm{d}^3r$$

$$\rho \int \bar{G}^i J(0)G^i(\boldsymbol{r})' J(-\boldsymbol{r})\mathrm{d}^3r$$

$$\rho \int G^i(\boldsymbol{r}) J(0)\bar{G}^{i\prime} J(-\boldsymbol{r})\mathrm{d}^3r$$

$$\rho \int \bar{G}^i J(r) G^i(-r)' J(0) \mathrm{d}^3 r$$

$$\rho \int G^i(r) J(-r) \bar{G}^{i\prime} J(0) \mathrm{d}^3 r$$

$$\rho \int G^i(r) J(0) A^i(-r) J(0) \mathrm{d}^3 r$$

In terms containing $G(r)$ the pair distribution g(r) does not occur explicitly because $G(r)$ already contains it as a factor. For the same reason one has to use the modified Green function A in the last of the two centre terms.

• three centre terms:

$$\rho^2 \int \int G^i(r)(gJ)(r')\bar{G}^{i\prime}(gJ)(-r-r')\mathrm{d}^3 r \mathrm{d}^3 r'$$

$$\rho^2 \int \int G^i(r)(gJ)(r')G^i(-r-r')'J(0)\mathrm{d}^3 r \mathrm{d}^3 r'$$

$$\rho^2 \int \int G^i(r)J(0)G^i(r')'(gJ)(-r-r')\mathrm{d}^3 r \mathrm{d}^3 r'$$

$$\rho^2 \int \int \bar{G}^i(gJ)(r)G^i(r')'(gJ)(-r-r')\mathrm{d}^3 r \mathrm{d}^3 r'$$

$$\rho^2 \int \int G^i(r)J(-r)G^i(r')'J(-r')g(|r-r'|)\mathrm{d}^3 r \mathrm{d}^3 r'$$

where $(gJ)(r) = g(r)J(r)$.

• four centre term:

$$\rho^3 \int \int \int G^i(r)(gJ)(r')G^i(r'')'(gJ)(-r-r'-r'')\mathrm{d}^3 r \mathrm{d}^3 r' \mathrm{d}^3 r''$$

$$+\rho^3 \int \int \int G^i(r)(gJ)(r')G^i(r'')'(gJ)(-r-r'-r'')h(|r+r'|)\mathrm{d}^3 r \mathrm{d}^3 r' \mathrm{d}^3 r''$$

$$+\rho^3 \int \int \int G^i(r)(gJ)(r')G^i(r'')'(gJ)(-r-r'-r'')h(|r'+r''|)\mathrm{d}^3 r \mathrm{d}^3 r' \mathrm{d}^3 r''$$

In general, at each type of atom more than one basis orbital has to be taken into account. As mentioned above, one has to build a fourfold sum running through the orbital types. The effect of doing this can be described in the following manner: The products listed above have to be interpreted as matrix products of G and J (running through the different orbitals at each atom) and the trace over the result has to be inserted for the term in square brackets in (2).

3. Angular dependence and Fourier transforms of the current matrix elements

Especially for evaluating the three and four centre terms above, it is very useful to change into the Fourier space, because all folding integrals become simple products there. The matrix elements of the Green functions as well as those of the current are in general not spherically symmetric but depend on all three space coordinates. As for the Green function in the sp^3- or sp^3d^5-fluid model [32, 33], one can introduce angular variables for the orbital directions (denoted, e.g., by $\hat{s}$, meaning the unit vector of the direction as well as two of the Euler angles). After all needed transformations, the average over these angular variables can be taken. In

addition, one has to introduce a third angular variable for the direction of the electrical field of the light E (which determines the component of the current vector). Notice that the E-angle variables appearing in each of the two J-components in the terms in (2) are the same (so they are not uncorrelated). Similar to the procedure and the terminology in [33] (as far as possible we also take the same notations as in [33]) one now deals with orbitals 'with direction $\hat{s}$'—that are orbitals which have the angular dependence $Y_0^l(\hat{r}')$ in a reference frame where the z-axis is parallel to the direction $\hat{s}$ in the laboratory system. Choosing a laboratory system where the z axis is parallel to the distance vector between the two atoms considered r (i.e. $r = r\hat{z}$) the matrix elements of the current in the direction of E between two orbitals with orbital quantum numbers l_1, l_2 and directions $\hat{s}_1$, $\hat{s}_2$ can be expanded in terms of (totally normalized) spherical harmonics:

$$J_{l_1,l_2}(r\hat{z}, \hat{s}_1, \hat{s}_2, \hat{s}_E) = \sum_{\nu_1,\nu_2,\nu_E} J_{\nu_1\nu_2\nu_E}^{l_1l_2}(r)Y_{\nu_1}^{l_1}(\hat{s}_1)Y_{\nu_2}^{l_2}(\hat{s}_2)Y_{\nu_E}^1(\hat{s}_E). \tag{3}$$

Only terms with $\nu_E = -\nu_1 - \nu_2$ do not vanish (see appendix) consistent with the dipole selection rule. An analogous expansion holds for the Fourier transformed function $\tilde{J}$, where the orientations $\hat{s}_1'$, $\hat{s}_2'$, $\hat{s}_E'$ now have to be considered in a laboratory frame where the z axis is parallel to the actual k vector. So the transformation of the coefficients in J to that in $\tilde{J}$ can be performed in two steps: first, a rotation of the reference frame and, second, the Fourier transformation, which may be performed by the use of the Rayleigh expansion of the exponential factor [34] yielding some Fourier–Bessel transformations. Details and the resulting transformation formulas for s and p-like states are given in the appendix.

As an example the first of the above listed three centre terms W_1^3 for a sp^3-liquid is now treated. For abbreviation, $I = (gJ)$ is used and we suppress the index i for the imaginary part. As already mentioned, the functions G and I are matrices because of the different orbitals at each atom, and we evaluate the integral in Fourier space. Instead of summing over the three possible directions of the p-orbitals at each atom, the convolution property given in equation (3.9) of [32] (or more generally in [33]) can be used in a similar way as used there. The final result for the term considered is:

$$W_1^3 = \frac{\rho^2}{(2\pi)^3} \sum_{l_1,l_2,l_3=0}^{1} 3(2l_1+1)(2l_2+2)(2l_3+1) \int\int\int\int\int$$

$$\times \tilde{G}^{l_1l_2}(k, \hat{s}_1, \hat{s}_2)\tilde{I}^{l_2l_3}(k, \hat{s}_2, \hat{s}_3, \hat{s}_E)\bar{G}^{l_3}\tilde{I}^{l_3l_1}(k, \hat{s}_3, \hat{s}_1)\frac{d^2\hat{s}_1}{4\pi}\frac{d^2\hat{s}_2}{4\pi}\frac{d^2\hat{s}_3}{4\pi}\frac{d^2\hat{s}_E}{4\pi}d^3k$$

$$= \frac{\rho^2}{2\pi^2} \sum_{l_1,l_2,l_3=0}^{1} 3(2l_1+1)(2l_2+2)(2l_3+1)$$

$$\times \sum_{\nu,\mu}(-1)^\mu \int_0^\infty \tilde{G}_{l_1l_2\nu}(k)\tilde{I}_{\nu,\mu,-\nu-\mu}^{l_2l_3}(k)\bar{G}_{l_3}\tilde{I}_{-\mu,-\nu,\mu+\nu}^{l_3l_1}(k)dk.$$

The factor $(-1)^\mu$ is due to the complex definition of spherical harmonics $Y_\mu^{l*} = (-1)^\mu Y_{-\mu}^l$ and the non-diagonal Green function terms are given by the expansion [32, 33]:

$$\tilde{G}^{l_1l_2}(k\hat{z}, \hat{s}_1, \hat{s}_2) = \sum_\mu \tilde{G}_{l_1l_2\mu}(k)Y_\mu^{l_1}(\hat{s}_1)Y_{-\mu}^{l_2}(\hat{s}_2)$$

The other terms needed can be calculated in a similar way, but some helpful remarks are necessary. For the evaluation of the four-centre-term part with the interconnecting h term, one has to compute the folding integral of two terms in the Fourier space, transform it back to real space, multiply it with $h(r)$ and proceed then as with the three centre terms. If one decides to evaluate the two centre terms in real space (for reduction of computational cost) one has to

pay attention to the change of sign by using, e.g., $G^{l_1,l_2}(\boldsymbol{r}, \hat{\boldsymbol{s}}_1, \hat{\boldsymbol{s}}_2)$ instead of $G^{l_1,l_2}(-\boldsymbol{r}, \hat{\boldsymbol{s}}_1, \hat{\boldsymbol{s}}_2)$. Then an additional factor appears, $(-1)^{l_1+l_2}$ in case G is reversed and $(-1)^{l_1+l_2+1}$ in case J is reversed.

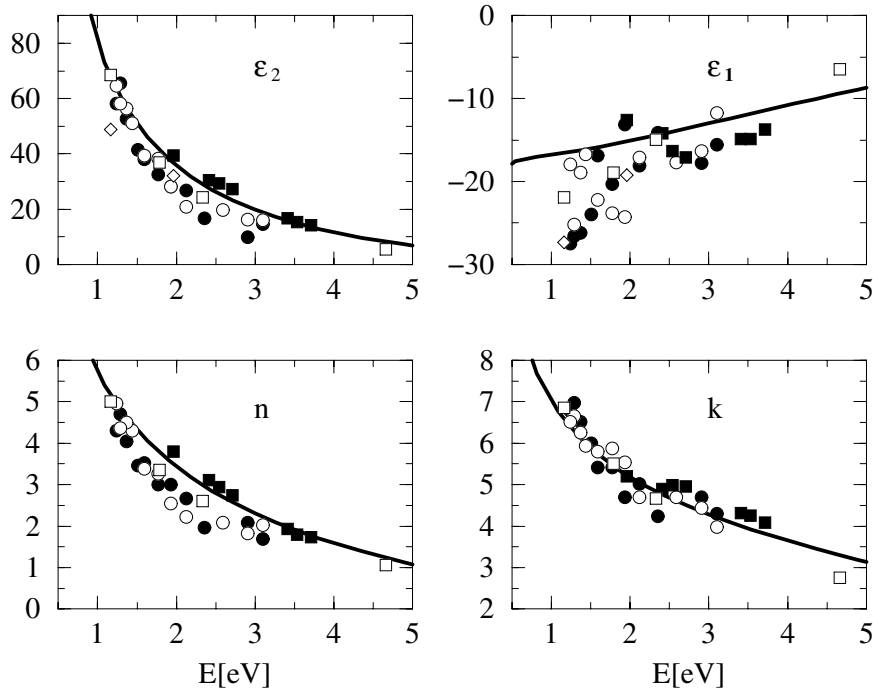## 4. Optical properties of liquid silicon

For the determination of the underlying electronic properties, e.g., the ensemble-averaged Green functions, the following parameters were used: the tight binding parameters are the often used ones published by Goodwin, Skinner and Pettifor [35] describing a basis of 3s- and 3p-orbitals. The pair distribution function was taken from the experimental data of Waseda *et al* [36] and the mass density $\rho_m = 2.59$ g cm^{-3} we take from [37]. The integral equations of the SSCA/EMA are then solved on a (one dimensional) grid for the atomic distance of 4096 points and a spacing of 0.05 a_B (Bohr radius). The resulting electronic density of states is given in [33]. It is similar to that one in [8]. One question arising when using empirical parameters (see above) is how to get the current (respectively, the momentum or optical) matrix elements. Since there is no consistent way to obtain these from the empirical parameters, especially if these do not contain any overlap, we evaluate them from the simple atomic Slater-orbital fits given by Clementi and Raimondy [38]. The formulas are given in the appendix and first lead to the elements in Fourier space which are then transformed back to real space.
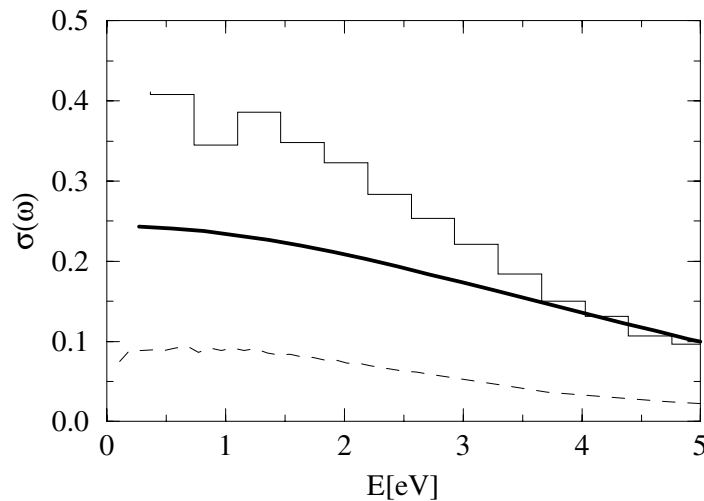
Figure 1. Optical conductivity of liquid silicon in a.u.'s $(e^2/\hbar a_B = 4.6 \times 10^6 (\Omega m)^{-1})$. Result from Green function method ——, molecular dynamics data from [2] —— and from [1] - - - -.

With these Green functions and current matrix elements the terms given in part 2 are computed, and one immediately gets the optical (that is the frequency dependent) conductivity from (2). The result is shown in figure 1 together with the only two results, to our knowledge, from molecular dynamics simulations [1, 2]. These deviate in the low-frequency region (less about 2 eV) from our results by a factor of about 0.3 or 1.5 respectively. The imaginary part of the dielectric function is given by $\varepsilon_2(\omega) = \sigma(\omega)/(\varepsilon_0\omega)$. To get the real part, one has to carry out a Kramers–Kronig transformation. Unfortunately, the restriction to the 3s and 3p states leads to a sudden (unphysical) decrease and vanishing of the conductivity (above about 5 eV) due to the artificial right band edge in the density of states in the sp^3-model [8, 33].

Therefore, an empirical extrapolation is needed for a useful evaluation of the Kramers–Kronig transformation. We use an extrapolation $\sim \omega^{-3}$ for $\varepsilon_2(\omega)$ above 5 eV corresponding to a Drude behaviour at high energies. The choice of the extrapolation scheme (within a physically reasonable frame) does not affect the low-frequency (less than about 3 eV) values of ε_1 very strongly. The total contribution of the extrapolated part to ε_1 is less than about 0.8 in this regime—much less than the corresponding absolute value of ε_1.


Figure 2. Complex dielectric function ($\varepsilon_1 + i\varepsilon_2$) and complex index of refraction ($n + ik$) of liquid silicon. Result from continuum Green function method ——, experimental data from [14]●($T = 1450$ K), [14]○($T = 1600$ K), [12]■, [39]□, and [16, 17]◇.

The resulting optical properties (complex dielectric function $\varepsilon_1 + i\varepsilon_2$ and complex index of refraction $n + ik$) are shown in figure 2 together with some experimental data from the literature. The overall agreement in the complex index of refraction and the imaginary part of the dielectric function is very good. The molecular dynamics results mentioned above lead to values of ε_2 ($\sim \sigma/\omega$) that deviate by an factor 0.3 or 1.5 respectively in the low-frequency region and are therefore not more satisfying compared to the experiments than our results. Deviations of our results appear in the real part of the dielectric function—but there we also find a large fluctuation of the experimental values. This is because $\varepsilon_1 = n^2 - k^2$ is here a relatively small difference of two large values resulting in a large error. Nevertheless, we find the tendency of our computed ε_1 to be not as negative as the experimental values in the low-energy regime. The other properties fit very well and are dominated by the metallic behaviour which is given by the factor $1/\omega$ in ε_2.

Because liquid silicon has a metallic character, it is appropriate to attempt an approximation of the optical properties by a Drude model. The data found from a fit of the function $\sigma_D = \varepsilon_0 \omega_p^2 \tau/(\omega^2 \tau^2 + 1)$ to the result of the continuum Green function method (not taking

M S Fuchs

into account the extrapolated part) are the plasma frequency $\omega_p = 2.87 \times 10^6$ rad s^{-1} and the relaxation time $\tau = 0.159$ fs. Compared with values found experimentally (e.g., 2.5×10^6 rad s^{-1}, 0.212 fs [17]), it is obvious that the relaxation time is somewhat too small. This is consistent with the deviations found in the low-energy part for the real part of the dielectric function as one may see from the Drude equation $\varepsilon_1 = 1 - \omega_p^2 / (\omega^2 + \tau^{-2})$ where the second (negative) part scales approximately with τ^2 at low frequencies. Because the relaxation time determines the decreasing behaviour of σ with increasing ω in the framework of the Drude model $(\sigma_D(\omega)/\sigma_D(0) = 1/(\omega^2\tau^2 + 1))$ we can conclude that the optical conductivity found here decreases too slowly. That is neither a consequence of using the continuum Green function method nor of the neglected vertex corrections but rather of the limitations of the sp^3-model. This can be shown in terms of joint densities of states (JDOS $D(E) = \int_{E_F-E}^{E_F} n(E')n(E' + E)\mathrm{d}E'$, E_F Fermi energy, $n(E)$ electronic density of states) divided by the energy. Because the conductivity is a JDOS per energy weighted with optical matrix elements we may draw conclusions about the conductivity itself from the JDOS per energy. For the reasons given above we are interested in the decreasing behaviour of that JDOS per energy and therefore the slopes of this function are shown in figure 3 for the sp^3-and the sp^{3}d^5-model. At low energies the sp^{3}d^5 slope is almost zero, i.e. the JDOS per enery is constant, whereas the sp^3 slope is positive, i.e. the JDOS per energy is even increasing. This is caused by the superlinear increase of the electronic density of states in the sp^3-model in the region near the Fermi enery. The sudden decrease in the JDOS (large negative slope) in the sp^3-model above about 6 eV, however, is only a consequence of the artificial right band edge in the density of states. The beginning of a steeper negative slope in the sp^{3}d^5-model in contrast is due to the dip in the occupied part of the density of states between p- and s-dominated states [33]. The almost constant behaviour at low energies is typical for a simple metal whereas the features of the sp^{3}model seem in fact not very well suited for a description within the Drude model.
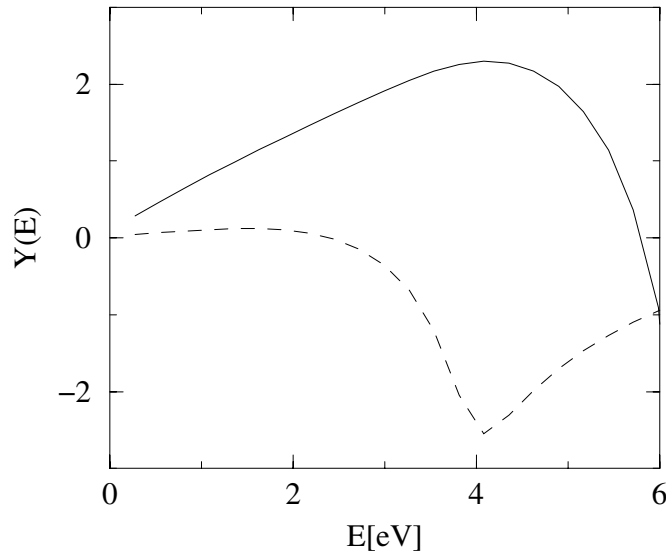
Figure 3. Slope Y(E) of the JDOS per energy for the sp^3-model —— and for the sp^{3}d^5-model - - - -.

$$\left(Y(E) = \mathrm{d}/\mathrm{d}E \left(\int_{E_F-E}^{E_F} \mathrm{d}E' n(E')n(E + E')/E \right) \right)$$

However, if the conductivity is fitted to the Drude model the decreasing behaviour of the corresponding JDOS per energy influences (besides the effect of the optical matrix elements) the resulting relaxation time. Therefore we conclude from the reduction of the slope of the JDOS per energy when using the sp^3d^5-model the slope of the conductivity up to about 5 eV will also become reduced (i.e. more negative) and the results for the Drude parameters as well as for the real part of the dielectric function are expected to become better in the sp^3d^5-model.

A calculation of the optical properties in the sp^3d^5-model going beyond the above given estimation demands further extensions or generalizations of the formulae (e.g., the transformation rules given in the appendix) and might be the aim of a separate paper.

5. Conclusions

The results of the integral equation approach to the electronic properties of liquid silicon as a sp^3-fluid were used to evaluate the optical properties. To do this we first considered the terms needed for an approximation of the optical conductivity consistent with the SSCA/EMA. Second, we extended the method for the effective handling of the angular dependences known from the molecular liquid model to the direction of the electrical field of the incoming light. The computed complex index of refraction and the imaginary part of the dielectric function—even in the sp^3-model—agree well with experimental data. Deviations occurring in the real part of the dielectric function and the fitted Drude parameters are shown to be an artifact of the sp^3-model.

Appendix A. Evaluating and transforming current matrix elements

The evaluation of the matrix elements of the current (or, equivalently, of the momentum) between two orbitals ϕ and ψ is best done in Fourier space

$$
\begin{aligned}
e_E \cdot \tilde{J}(k) = e_E \cdot &\int d^3R \left(\left\langle \phi(r) | ih\frac{e}{m}\nabla_r \psi(r-R) \right\rangle_r \exp(ik \cdot R) \right) \\
= &- ih\frac{e}{m} e_E \cdot \int d^3r \left(\tilde{\phi}(r) \int d^3R \left(\nabla_r \psi^*(R) \exp(ik \cdot (-R+r)) \right) \right) \\
= &\, \tilde{\phi}(k) h\frac{e}{m} e_E \cdot k \tilde{\psi}^*(k).
\end{aligned}
\tag{A.1}
$$

Following from that, the angular dependence of the direction of the electrical field is given here by $Y_0^1(\hat{s}_E)$. Of course, the restriction $l_E = 1$ is just a consequence of the dipole approximation.

The Fourier transformed orbitals can be evaluated by using the Rayleigh expansion for the $\exp(ik \cdot r)$ factor, resulting in

$$
\tilde{\psi}(k) = \int d^3r u_\psi(r) Y_\mu^m(\hat{r}) \exp(ik \cdot r) = 4\pi i^m \int dr r^2 j_m(kr) u_\psi(r) Y_\mu^m(\hat{k})
$$

and, consequently, for an orbital with direction $\hat{s}_1$ one finds in a reference frame with $\hat{z} \parallel k$

$$
\tilde{\psi}_{\hat{s}_1}(k) = 4\pi i^m \int dr r^2 j_m(kr) u_\psi(r) Y_0^m(\hat{s}_1)
$$

Therefore, in the expansion of $\tilde{J}$ (analogous to (3)) only terms with $\nu_1 = 0$, $\nu_2 = 0$, $\nu_E = 0$ appear.

The three-dimensional Fourier transforms of (3) can be obtained via some one-dimensional Fourier–Bessel transformations, similar to the procedure in [32]. To find the connections between the functions, their Fourier transforms and the functions which have to be Fourier–Bessel transformed, one can, in general, proceed in the following manner. Remember that

(3) holds for a reference system with z axis parallel to the interconnecting vector $\mathbf{R}$ and the analogous expansion in k-space for a reference frame with z axis parallel to the actual $\mathbf{k}$. Therefore, one has first to rotate the reference system (from $z \parallel \mathbf{R}$ to $z \parallel \mathbf{k}$). In practice that means that all spherical harmonics are replaced by sums over rotation matrices times spherical harmonics in the new frame [40]. Now one can use the Rayleigh-expansion for $\exp(i\mathbf{k} \cdot \mathbf{R})$ (e.g. [34]) to obtain the Fourier transformation itself. The main thing to do is (lengthy but straight-forward) to evaluate all coefficients and sort the terms. We present here the result for s- and p-states only:

$$\tilde{J}_{0,0,0}^{0,0} = \left(J_{0,0,0}^{0,0} \right)^{(1)}$$

$$\tilde{J}_{0,0,0}^{1,0} = \frac{1}{3} \left(J_{0,0,0}^{1,0} - 2J_{1,0,-1}^{1,0} \right)^{(0)} + \frac{2}{3} \left(J_{0,0,0}^{1,0} + J_{1,0,-1}^{1,0} \right)^{(2)}$$

$$\tilde{J}_{1,0,-1}^{1,0} = J_{-1,0,1}^{1,0}$$

$$= -\frac{1}{3} \left(J_{0,0,0}^{1,0} - 2J_{1,0,-1}^{1,0} \right)^{(0)} + \frac{1}{3} \left(J_{0,0,0}^{1,0} + J_{1,0,-1}^{1,0} \right)^{(2)}$$

$$\tilde{J}_{0,0,0}^{1,1} = \frac{3}{5} \left(J_{0,0,0}^{1,1} - 2J_{1,-1,0}^{1,1} \right)^{(1)} + \frac{2}{5} \left(J_{0,0,0}^{1,1} + 3J_{1,-1,0}^{1,1} \right)^{(3)}$$

$$\tilde{J}_{0,0,0}^{1,1} = \frac{1}{5} \left(3J_{0,0,0}^{1,1} - 2J_{0,1,-1}^{1,1} - 2J_{1,0,-1}^{1,1} - 2J_{1,-1,0}^{1,1} \right)^{(1)}$$
$$+ \frac{2}{5} \left(J_{0,0,0}^{1,1} + J_{0,1,-1}^{1,1} + J_{1,0,-1}^{1,1} + J_{1,-1,0}^{1,1} \right)^{(3)}$$

$$\tilde{J}_{0,1,-1}^{1,1} = \tilde{J}_{0,-1,1}^{1,1} \qquad\qquad\qquad\qquad\qquad\qquad\qquad\qquad \text{(A.2)}$$
$$= -\frac{1}{5} \left(J_{0,0,0}^{1,1} - 4J_{0,1,-1}^{1,1} + J_{1,0,-1}^{1,1} + J_{1,-1,0}^{1,1} \right)^{(1)}$$
$$+ \frac{1}{5} \left(J_{0,0,0}^{1,1} + J_{0,1,-1}^{1,1} + J_{1,0,-1}^{1,1} + J_{1,-1,0}^{1,1} \right)^{(3)}$$

$$\tilde{J}_{1,0,-1}^{1,1} = \tilde{J}_{-1,0,1}^{1,1}$$
$$= -\frac{1}{5} \left(J_{0,0,0}^{1,1} + J_{0,1,-1}^{1,1} - 4J_{1,0,-1}^{1,1} + J_{1,-1,0}^{1,1} \right)^{(1)}$$
$$+ \frac{1}{5} \left(J_{0,0,0}^{1,1} + J_{0,1,-1}^{1,1} + J_{1,0,-1}^{1,1} + J_{1,-1,0}^{1,1} \right)^{(3)}$$

$$\tilde{J}_{1,-1,0}^{1,1} = \tilde{J}_{-1,1,0}^{1,1}$$
$$= -\frac{1}{5} \left(J_{0,0,0}^{1,1} + J_{0,1,-1}^{1,1} + J_{1,0,-1}^{1,1} - 4J_{1,-1,0}^{1,1} \right)^{(1)}$$
$$+ \frac{1}{5} \left(J_{0,0,0}^{1,1} + J_{0,1,-1}^{1,1} + J_{1,0,-1}^{1,1} + J_{1,-1,0}^{1,1} \right)^{(3)}.$$

The upper numerals in parentheses on the right denote the corresponding Fourier–Bessel transformation [32, 41]. The inverse transformation is analogous (interchange of J and $\tilde{J}$). One finds that only terms with $\nu_1 + \nu_2 + \nu_E = 0$ occur, a consequence of the dipole selection rule. For the *pure* current element, the formulas simplify a little because of symmetry, i.e. starting only with terms $\tilde{J}_{000}^{lm}$ (see above) it follows that $J_{1,-1,0}^{1,1} = J_{-1,1,0}^{1,1} = J_{1,0,-1}^{1,1} = J_{-1,0,1}^{1,1} = J_{0,1,-1}^{1,1} = J_{0,-1,1}^{1,1}$. Unfortunately, not only the *pure J* and its transformation is needed but also *J* weighted with the pair distribution function.

Acknowledgments

References

[1] Allen P B and Broughton J Q 1987 *J. Chem. Phys.* **91** 4964
[2] Štich I, Car R and Parrinello M 1991 *Phys. Rev.* B **44** 4262
[3] Chelikowsky J R, Troullier N and Binggeli N 1994 *Phys. Rev.* B **49** 114
[4] Jank W and Hafner J 1990 *Phys. Rev.* B **41** 1497
[5] Kim E and Lee Y H 1994 *Phys. Rev.* B **49** 1743
[6] Klein P, Urbassek H M and Frauenheim T 1999 *Comp. Mater. Sci.* **13** 252
[7] Krajčí M and Hafner J 1995 *Phys. Rev. Lett.* **74** 5100
[8] López-Martín J-L, Lomba E, Kahl G, Winn M. D and Rassinger M 1997 *J. Phys.: Condens. Matter* **9** 3321
[9] Virkkunen R, Laasonen K and Nieminen R M 1991 *J. Phys.: Condens. Matter* **3** 7455
[10] Ivlev G D and Gatskevich E I 1996 *Semicond.* **30** 1093
[11] Jellison Jr G E and Lowndes D H 1985 *Appl. Phys. Lett.* **47** 718
[12] Jellison Jr G E and Lowndes D H 1987 *Appl. Phys. Lett.* **51** 352
[13] Krishnan S, Weber J K R, Nordine P C, Schiffman R A, Hauge R H and Margrave J L 1991 *High Temp. Sci.* **30** 137
[14] Shvarev K M, Baum B A and Gel'd P V 1975 *Sov. Phys. Solid State* **16** 2111
[15] Lampert M O, Koebel J M and Siffert P 1981 *J. Appl. Phys.* **52** 4975
[16] Li K D and Fauchet P M 1987 *Solid State Commun.* **61** 207
[17] Li K D and Fauchet P M 1987 *Appl. Phys. Lett.* **51** 1747
[18] Takasuka E, Tokizaki E, Terashima K and Kimura S 1995 *Appl. Phys. Lett.* **67** 152
[19] Takasuka E, Tokizaki E, Terashima K and Kimura S 1997 *J. Appl. Phys.* **81** 6384
[20] Ganter G, Boyen H G and Oelhafen P 163 *Europhys. Lett.* **31** 1995
[21] Ganter G, Boyen H-G and Oelhafen P 1996 *J. Non-Cryst. Sol.* **205–207** 490
[22] Hague C F, Sénémaud C and Ostrowoecki H 1980 *J. Phys. F: Metal Phys.* **10** L267
[23] Winn M D and Logan D E 1989 *J. Phys.: Condens. Matter* **1** 1753
[24] Winn M D and Logan D E 1989 *J. Phys.: Condens. Matter* **1** 8683
[25] Matsubara T and Toyozawa Y 1961 *Prog. Theor. Phys.* **26** 739
[26] Movaghar B and Sauer G W 1979 *J. Phys. F: Metal Phys.* **9** 867
[27] Zhang X-G and Butler W H 1995 *Phys. Rev.* B **51** 10085
[28] Roth L M and Singh V A 1980 *J. Physique Suppl.* **8** C8–459
[29] Roth L M and Singh V A 1982 *Phys. Rev.* B **25** 2522
[30] Rubio J 1969 *J. Phys. Chem.* **2** 288
[31] Roth L M 1976 *J. Phys. F: Metal Phys.* **6** 2267
[32] Lomba E, López-Martín J L and Kahl G 1996 *J. Chem. Phys.* **105** 7735
[33] Fuchs M S K 2000 *J. Phys.: Condens. Matter* **12** 1667
[34] Blum L 1972 *J. Chem. Phys.* **56** 303
[35] Goodwin L, Skinner A J and Pettifor D G 1989 *Europhys. Lett.* **9** 701
[36] Waseda Y, Shinoda K, Sugiyama K and Takeda S 1995 *Jpn. J. Appl. Phys.* **34** 4124
[37] Waseda Y 1980 *The Structure of Non-Crystalline Materials; Liquids and Amorphous Solids* (New York: McGraw-Hill)
[38] Clementi E and Raimondi D L 1963 *J. Chem. Phys.* **38** 2686
[39] Liu J M 1982 *Thermal model of picosecond laser interactions with silicon* Master's thesis Havard University Cambridge
[40] Edmonds A R 1996 *Angular momentum in quantum mechanics* (Princeton: Princeton University Press)
[41] Lado F 1982 *Mol. Phys.* **47** 283